

Land subsidence and uplift due to long-term groundwater extraction and artificial recharge in Shanghai, China

Yun Zhang¹ · Jichun Wu¹ · Yuqun Xue¹ · Zhecheng Wang¹ · Yiguang Yao¹ · Xuexin Yan² · Hanmei Wang²

Received: 31 January 2015 / Accepted: 31 July 2015 / Published online: 29 August 2015
© Springer-Verlag Berlin Heidelberg 2015

Abstract Increasing artificial water recharge and restriction on groundwater pumpage have caused land displacements in Shanghai (China) to shift from subsidence to uplift. On the basis of field and laboratory data, the characteristics and mechanism of land subsidence and uplift are analyzed and discussed. Under the condition of long-term groundwater extraction, the deformation of aquifer and aquitard units consists of elastic, plastic, visco-elastic, and visco-plastic components. The recoverable elastic and visco-elastic deformation is only a small portion of the total deformation for both aquitard and aquifer units, especially when the groundwater level in the units is lower than the historically lowest values. When the groundwater level in aquifer and aquitard units rises, whether their expansion occurs immediately or not, depends on the changing modes of groundwater level they have experienced. Even aquifer units do not always rebound closely following the rise of groundwater level in them. The lagging of the occurrence of arrested land subsidence and uplift, clearly behind the rise of groundwater level in aquifer units, can be attributed to the visco-plastic deformation of all units and the consolidation deformation of aquitard units. Artificial recharge and limitation of pumpage are efficient measures for controlling land subsidence, but

earlier actions are necessary to keep groundwater levels in all aquifer units above their historically lowest values all the time, if a more effective outcome is expected.

Keywords Groundwater extraction · Artificial recharge · Subsidence and uplift · Deformation · China

Introduction

Excessive groundwater extraction can cause groundwater level (pore water pressure) to decrease and effective stress to increase in hydrostratigraphic units. This can result in the compaction of the units, and land subsidence ensues. Many areas in the world have encountered severe land subsidence such as the Las Vegas Valley and the Santa Clara Valley in the United States (Galloway et al. 1999), Venice in Italy (Teatini et al. 2012), and Shanghai in China (Zhang and Wei 2005). Land subsidence can cause substantial damage such as loss of ground surface elevation, cracking of building foundations and underground pipelines, and intensification of storm tides in coastal areas.

In order to mitigate land subsidence, some measures have been taken to raise the groundwater level in hydrostratigraphic units such as water injection (artificial recharge) and banning or reducing pumping (Hoffmann et al. 2001; Kosloff et al. 1980; Chen et al. 2007). These measures are theoretically based on Terzaghi's effective stress principle. The effective stress in hydrostratigraphic units is decreased through increasing groundwater level, causing the units to expand. However, the outcome of costly artificial recharge is often not as effective as expected. Firstly, the magnitude of land uplift is usually much smaller than that of land subsidence even though groundwater in aquifers has recovered to its initial level. This is usually attributed to the plastic deformation of aquitard

✉ Yun Zhang
zhangyun@nju.edu.cn

¹ School of Earth Sciences and Engineering, Nanjing University, 163 Xianlin Avenue, Nanjing 210023, China

² Key Laboratory of Land Subsidence Monitoring and Prevention, Ministry of Land and Resources of China, Shanghai Institute of Geological Survey, 930 Lingshi Road, Shanghai 200072, China

units (Leake 1991). Secondly, field data have revealed that land subsidence did not cease but continued when the groundwater level in aquifers began to increase, and that land uplift often occurred after the groundwater level had risen for many years (Chen et al. 2007; Schmidt and Bürgmann 2003). This means that land uplift lags behind the rise of groundwater level in aquifers. It was usually thought that the recharged aquifer units deformed elastically and rebounded immediately when their groundwater level began to increase, and that the lagging of land uplift was ascribed to the consolidation of aquitards and other aquifers without recharge (Chen et al. 2007; Teatini et al. 2011), or the existence of clayey interbeds in recharge aquifers (Zhou and Burbey 2014). However, field data acquired from extensometer groups, which can provide the compaction of individual hydrostratigraphic units, suggest that aquifer units do not always behave as elastic materials and their deformation is sometimes irrecoverable; their expansion even lags behind the rising groundwater level in themselves, as it does in aquitard units (Zhang et al. 2012). The mechanisms of the regional land uplift by cessation or decrease of pumping and increase of artificial recharge are essentially unclear as yet, which has an adverse effect on the outcome of land subsidence mitigation; therefore, the focus of this paper is not on the spatial distribution of land subsidence and uplift but rather on its mechanisms. Based on newly updated long-term field and laboratory data, this paper aims to investigate the mechanisms of land subsidence and uplift in Shanghai and to discuss the effect of controlling

land subsidence by raising groundwater levels in aquifers.

Geological background and hydrogeological setting

Shanghai is a large metropolis located in the east of China (Fig. 1). The ground surface is low and flat, with the average elevation being approximately 4 m above the mean sea level. The thickness of the Quaternary deposits in Shanghai ranges from 100 m in the southwestern part to 400 m in the northern and eastern parts and averages 280 m. The depth contours of bedrock surface in Shanghai are shown in Fig. 2. The Quaternary deposits can be considered to be composed of six aquifers which consist mainly of medium-to-dense sands and sands with gravels. The uppermost is an unconfined aquifer and the other five are confined aquifers, which are denoted as A1–A5 from top to bottom in Fig. 3, respectively. In the southern Yangtse Delta region (including Shanghai and some areas of Jiangsu and Zhejiang provinces) the first and second aquifers are also called the first confined aquifer; thus, the third to fifth confined aquifers are called the second to fourth confined aquifers consecutively (Zhang et al. 2007). Between the aquifers are confining aquitards which consist mainly of clay and silty clay. The first aquitard is sub-divided into the first and second soft soil layers and the second hard soil layer, and the second aquitard is also called the third soft soil layer. The physical and mechanical properties of each unit are indicated in Table 1 (SGEAEB 2002; Zhang et al. 2003, 2007). The permeability of aquitard units is much weaker than that of

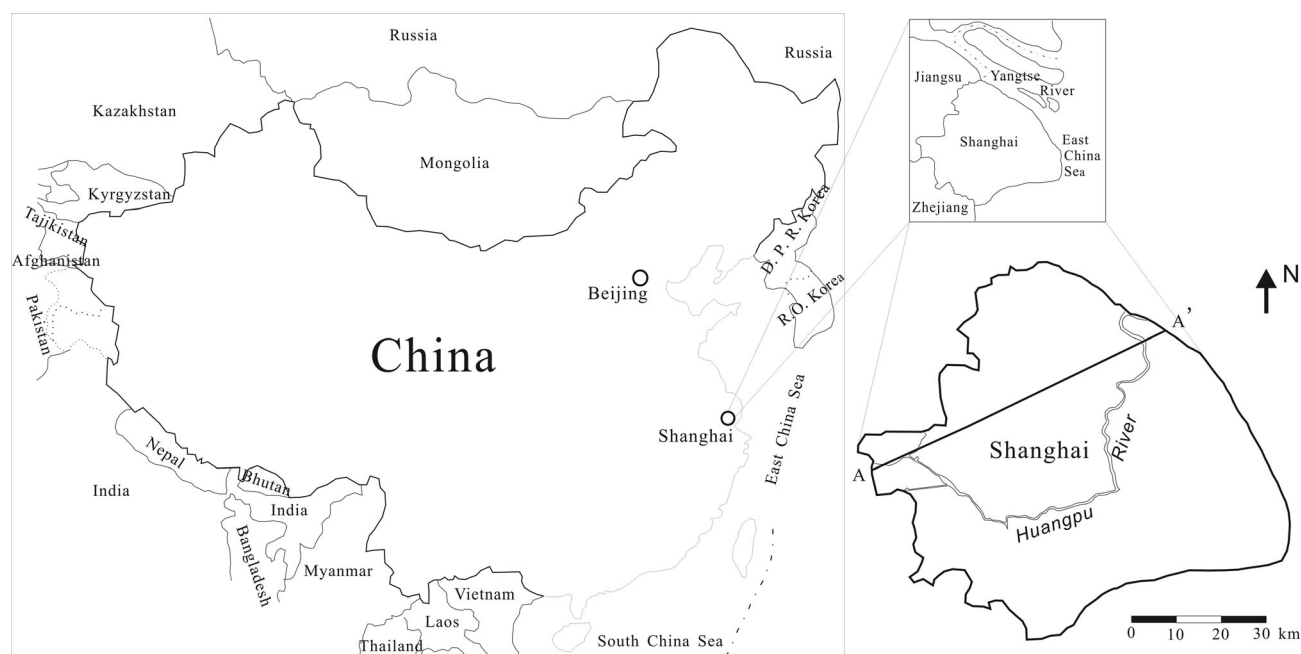
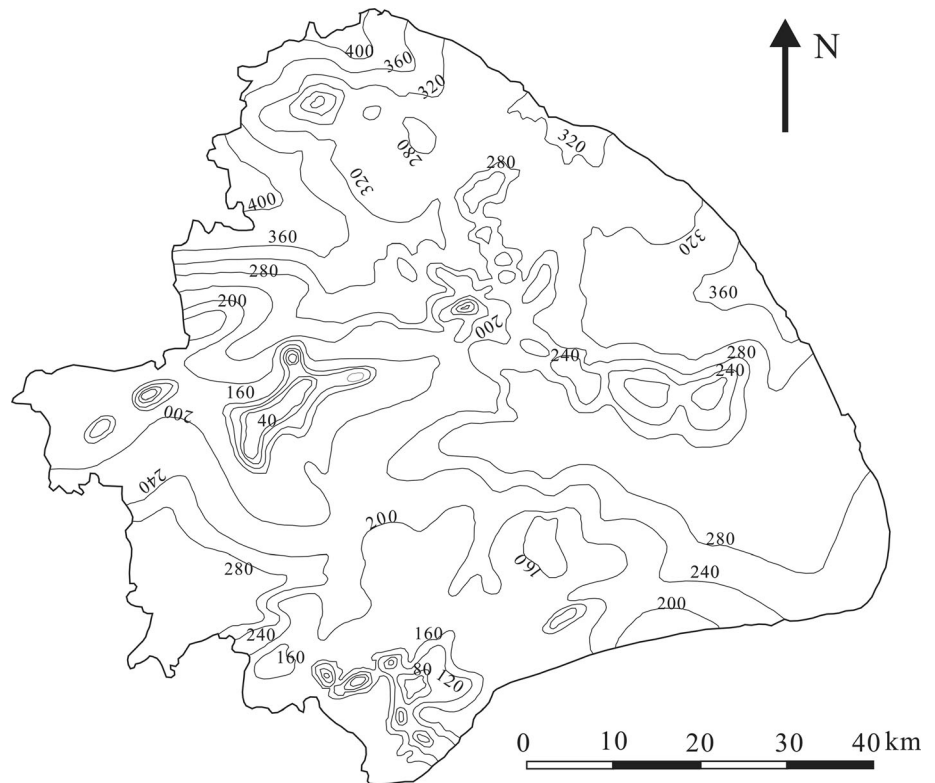


Fig. 1 Location of study area showing the position of hydrogeological cross section A–A'

Fig. 2 Depth contours of bedrock surface in Shanghai (unit: m) (modified from SGEAEB 2002)



aquifer units, and the three soft soil layers, especially the first one, are of high compressibility. The units should be fully saturated in situ. However, due to the loss of moisture in soil sample acquisition and transportation, the moisture content of soil samples measured in the laboratory may be smaller than that in situ, causing the values of the calculated degree of saturation to be less than 1.00, as shown in Table 1.

Groundwater extraction, artificial recharge, and resultant changes in groundwater level

Groundwater extraction in Shanghai dates back to 1860. The amount of pumpage was quite small before 1949, then it increased rapidly, especially in the late 1950s. The yearly

pumpage reached its peak of $2.03 \times 10^8 \text{ m}^3$ in 1963, as indicated in Fig. 4 (modified from Gong 2009). If only the urban area of Shanghai is considered, however, the yearly pumpage reached its peak of $1.39 \times 10^8 \text{ m}^3$ in 1958. Intensive groundwater extraction has caused severe land subsidence. During the period of 1957–1961, the average yearly rate of subsidence was 99.4 mm/year, with the maximum being up to 170 mm/year. In order to alleviate land subsidence, the amount of groundwater extraction was strictly limited and the yearly pumpage declined sharply to $0.59 \times 10^8 \text{ m}^3$ in 1968. Meanwhile, the exploited aquifers were gradually changed from the second and third confined aquifers to the fourth and fifth ones. As a result of the adjustment of mainly exploited aquifers and the restraint on groundwater extraction, the amount of pumpage from the second and third confined

Fig. 3 Conceptual hydrogeological cross section (A–A' in Fig. 1) of Shanghai (modified from SGEAEB 2002)

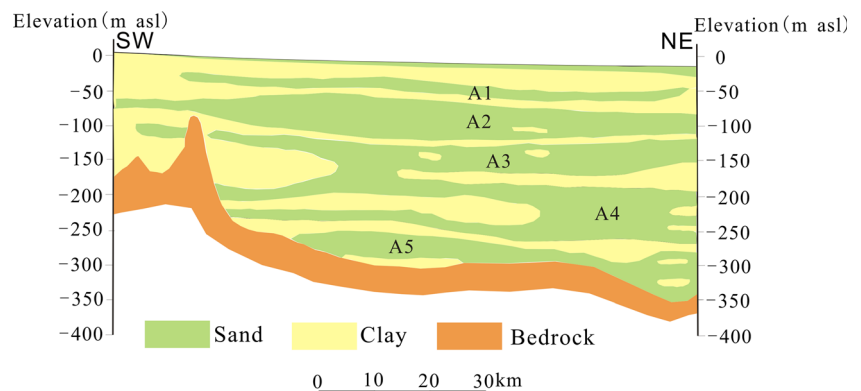


Table 1 Physical and mechanical properties of individual hydrostratigraphic units (data in *italics* pertain to aquifers)

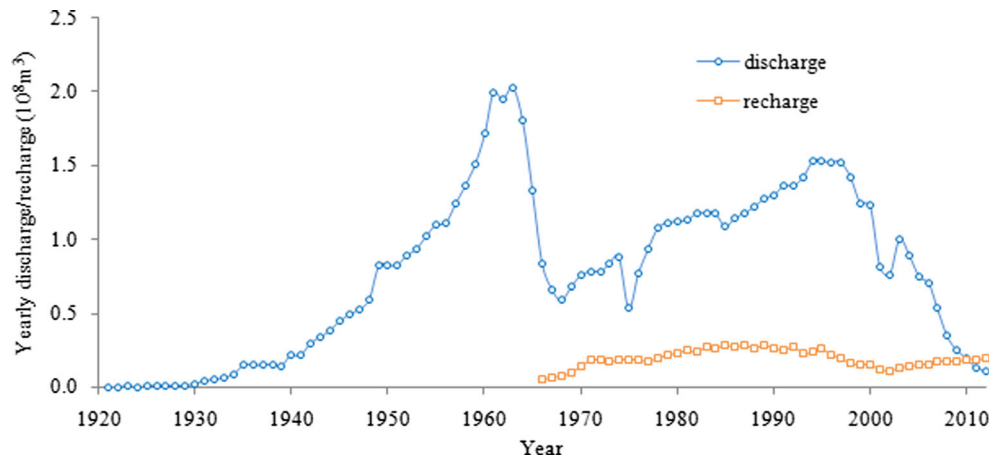
Hydrostratigraphic unit	Moisture content (%)	Unit weight (kN/m ³)	Void ratio	Degree of saturation (%)	State	Coefficient of compressibility (MPa ⁻¹)	Cohesion (kPa)	Internal friction angle (°)	Coefficient of permeability (10 ⁻⁷ cm/s)
Unconfined aquifer	26.0–43.0	17.6–19.3	0.75–1.17	81.0–89.8	Very loose to loose	0.29–0.40	6.0	22.0	21,500
1st aquitard: 1st soft soil layer	39.2–52.0	16.4–18.6	1.22–1.44	97.0–100	Soft plasticity–liquid	0.70–1.65	10.2	18.5	2.00
1st aquitard: 2nd soft soil layer	28.0–42.0	17.5–19.3	0.70–1.04	94.1–99.0	Soft–medium plasticity	0.40–0.71	17.1	20.7	1.34
1st aquitard: 2nd hard soil layer	22.7–25.2	19.1–20.5	0.66–0.70	95.1–98.9	Medium-hard plasticity	0.21–0.35	47.5	17.5	2.53
1st confined aquifer	21.2–27.1	19.1–20.1	0.63–0.81	91.2–91.5	Medium dense to dense	0.12–0.32	5.0	34.5	35,000
2nd aquitard (3rd soft soil layer)	26.1–38.2	18.2–19.3	0.78–1.08	90.9–100	Soft–medium plasticity	0.34–0.62	21.1	22.5	2.99
2nd confined aquifer	13.1–27.4	19.1–21.2	0.43–0.82	81.7–93.6	Medium dense to dense	0.26–0.45	0.0	38.1	41,000
3rd aquitard	23.9–30.0	19.7–20.5	0.66–0.86	92.1–100	Medium-hard plasticity	0.05–0.38	32.0	17.5	1.26
3rd confined aquifer	29.1–30.2	18.7–19.3	0.85–0.87	91.8–93.5	Medium dense	0.36–0.47	0.0	24.5	18,100
4th aquitard	17.0–32.3	19.1–21.4	0.51–0.90	90.6–99.0	Hard plasticity	0.07–0.25	45.0	16.0	0.13
4th confined aquifer	23.0–25.0	19.4–20.3	0.66–0.75	92.0–96.2	Loose to medium dense	0.25–0.63	0.0	27.8	34,300
5th aquitard	18.1–23.2	19.3–20.3	0.59–0.68	83.8–94.5	Hard plasticity	0.06–0.41	60.0	14.2	0.38
5th confined aquifer	27.8–30.2	18.8–19.1	0.80–0.91	92.0–97.8	Medium dense	0.26–0.43	0.0	27.5	17,900
6th aquitard	16.2–20.7	20.1–20.6	0.54–0.63	81.4–91.7	Hard plasticity–semisolid	0.12–0.36	30.0	21.0	0.30

aquifers decreased significantly, whereas that from the fourth and fifth confined aquifers increased gradually after 1968. However, the yearly pumpage increased again from the end of the 1970s to meet the domestic and industrial requirements for water, causing land subsidence to develop greatly once again. In order to prevent land subsidence from being exacerbated, the yearly pumpage has begun to decrease since 1998. On the other hand, artificial recharge in Shanghai started in 1966 and slightly increased in the following years (Fig. 4). In the period from 1983 to 1989, the yearly artificial recharge was nearly constant and approximately 0.27×10^8 m³/year. After that, the yearly recharge decreased slowly. However, it has increased year after year since 2003 and was first greater than the yearly discharge in 2011.

Changes in the amount of groundwater pumpage from and injection into the individual aquifers lead to different changing patterns of groundwater level in the individual confined aquifers. The typical groundwater level variations with time in the first to fifth confined aquifer are indicated in Fig. 5. The locations of these selected five observation wells are shown in Fig. 6. Groundwater levels in the first to third aquifers have similar changing patterns, whereby they reached their lowest values at the beginning of the 1960s and then rose rapidly because of the sharp decline in the amount of pumped groundwater from these aquifers. They increased to their highest values at the beginning of the 1970s and then fluctuated within a certain range, keeping the average nearly constant. After the middle of the 1980s, the groundwater levels began to decline slowly due to the slight increase in the amount of pumped groundwater, but they were much higher than their previous lowest values in the 1960s. Due to decreasing groundwater extraction and increasing water injection, the water level in these three aquifers has risen gradually since 1997.

The groundwater levels in the fourth and fifth confined aquifers have similar changing patterns. They declined slightly before 1965 and then rose rapidly due to the restraint on groundwater withdrawal, and almost remained at higher values after 1970 and fluctuated within a certain range. After the mid-1980s, the groundwater levels in the fourth and fifth aquifers began to decrease greatly due to the increasing amount of pumped groundwater, which was mainly extracted from these two aquifers. After 1990, the levels were lower than their historically lowest values in the 1960s. As a result of the decrease in the amount of exploited groundwater, the groundwater levels began to rise after 1998. The groundwater levels in the fourth and fifth confined aquifers have been rising greatly due to the strict limitation of pumpage and increasing injection since 2004. Consequently, the groundwater levels in the five confined aquifers in Shanghai do not simply maintain a monotonic falling or rising but change in complex patterns. The unconfined aquifer has been largely unexploited; thus, the groundwater level within it almost remains constant for the entire period.

Fig. 4 History of groundwater pumpage and artificial recharge in Shanghai



The evolution of groundwater levels in the aquifers from the very beginning of groundwater withdrawal to the present in Shanghai can be conceptualized into two modes: A and B, as shown in Fig. 7. Both modes have two decreasing and increasing cycles of groundwater level. The lowest groundwater level in the first cycle is lower than that in the second cycle for mode A, and the opposite case is true for mode B. The first to third confined aquifer units have experienced the changing mode of groundwater level like mode A, while the fourth and fifth aquifers have experienced that like mode B.

Land subsidence/uplift and deformation of individual hydrostratigraphic units

Excessive groundwater withdrawal has resulted in severe land subsidence in Shanghai, which was first reported in 1921. With a changing amount of pumpage and artificial recharge, the magnitude and rate of land subsidence changed correspondingly. Figure 8 shows the history of land subsidence in Shanghai, which can be separated into two phases: rapidly developing and controlling, including four and five stages, respectively, as indicated in Table 2. The average cumulative

Fig. 5 Typical variations of groundwater levels with time in different aquifer units. **a** The first, third and fourth aquifers; **b** The second and fifth aquifers

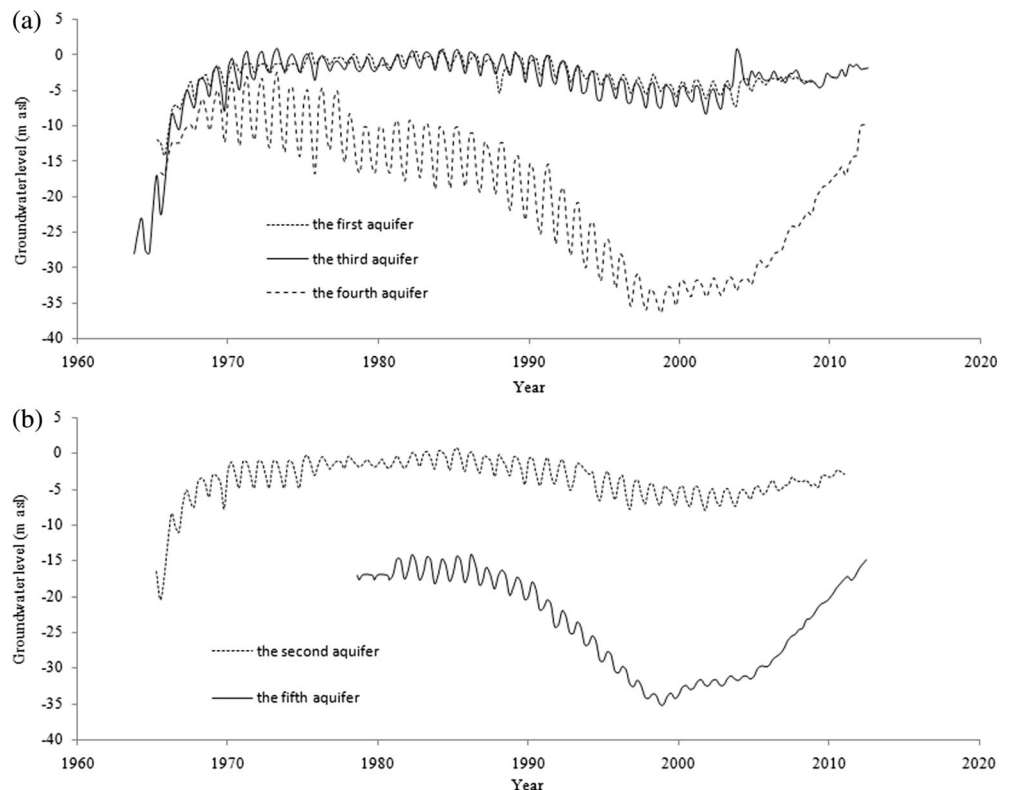
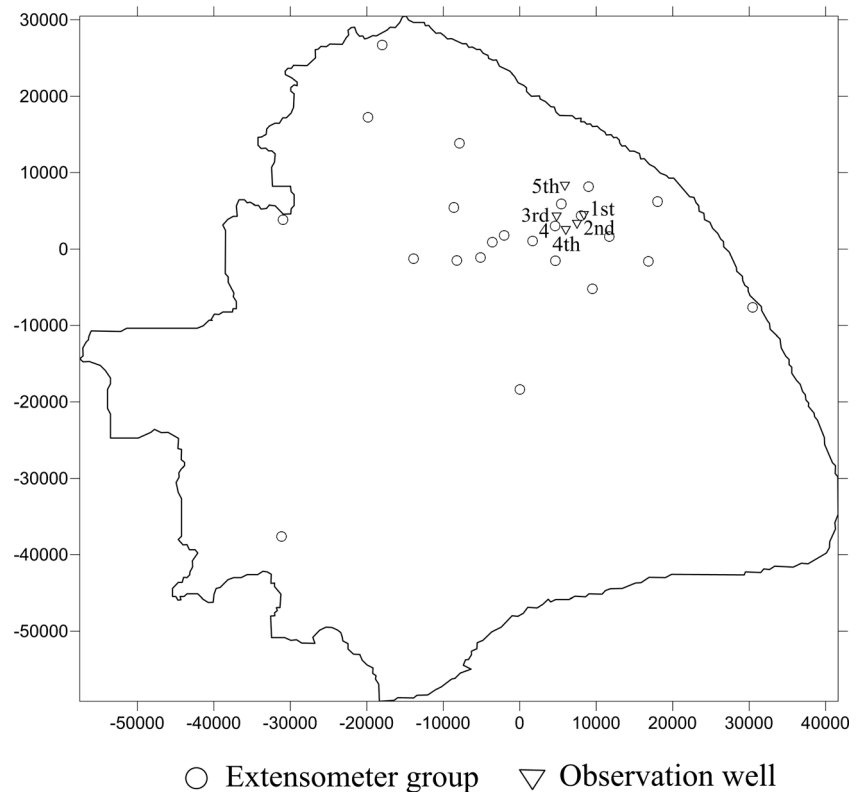


Fig. 6 Locations of extensometer groups and some of the observation wells in Shanghai (the unit of coordinates: m)



land subsidence was obtained through averaging the cumulative land subsidence measured at all benchmarks within the area of Shanghai. In phase 1 (before 1965), groundwater extraction was not restricted intentionally and land subsidence developed rapidly. The yearly rate of subsidence increased and reached the maximum in stage 3 (from 1957 to 1961). Then pumpage was dramatically reduced and groundwater level in all aquifers greatly increased till 1970; however, land subsidence was not arrested immediately but continued to increase at a slightly smaller rate. Land uplift did not occur until 1966. The occurrence of land uplift clearly lagged behind the beginning of groundwater level rising. In phase 2 (after 1965), groundwater extraction was limited in a planned way, and land subsidence was under control. The yearly subsidence

rate in this phase was much smaller than that in phase 1. Although groundwater pumpage had declined and groundwater level in aquifers had risen since 1998, land subsidence continued. As a whole, however, the subsidence rate has decreased and land surface is approaching a steady elevation, with the average yearly rate being 1.3 mm/year in the stage of 2009–2011. Compared with the change of groundwater levels in aquifers, the evolution of land subsidence lags behind the rise of groundwater level in aquifer units for both decreasing–increasing cycles.

In Shanghai, there are 25 extensometer groups which are anchored in the underlying bedrock. Some of them were built in the 1960s and have documented the compaction of individual hydrostratigraphic units since those years. Some were

Fig. 7 Conceptual modes of changing groundwater level in Shanghai

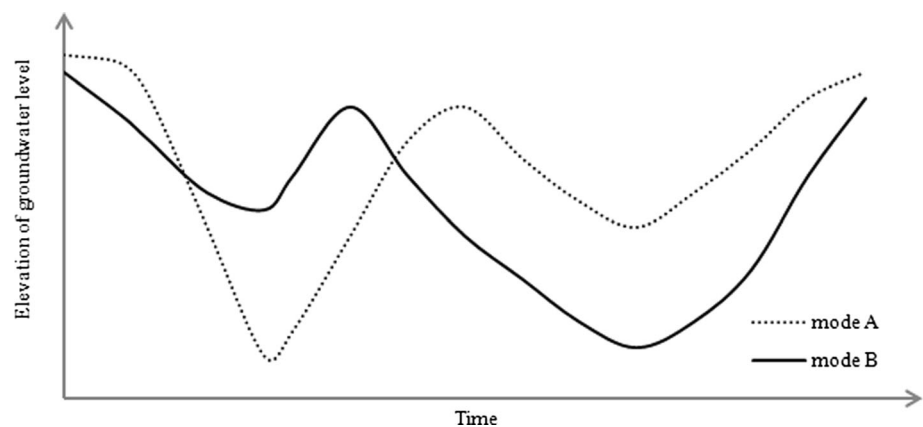
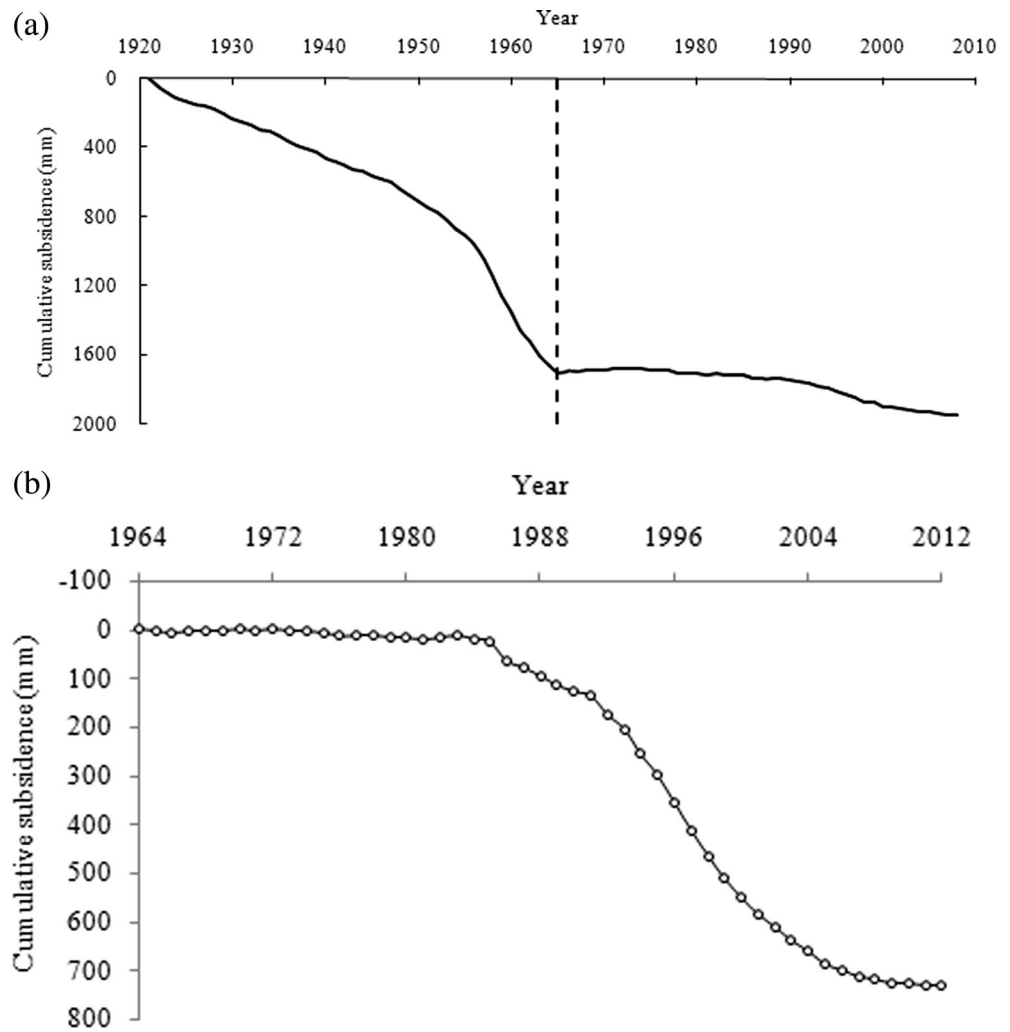


Fig. 8 History of land subsidence in Shanghai. **a** Average cumulative land subsidence; **b** cumulative subsidence at extensometer group 4



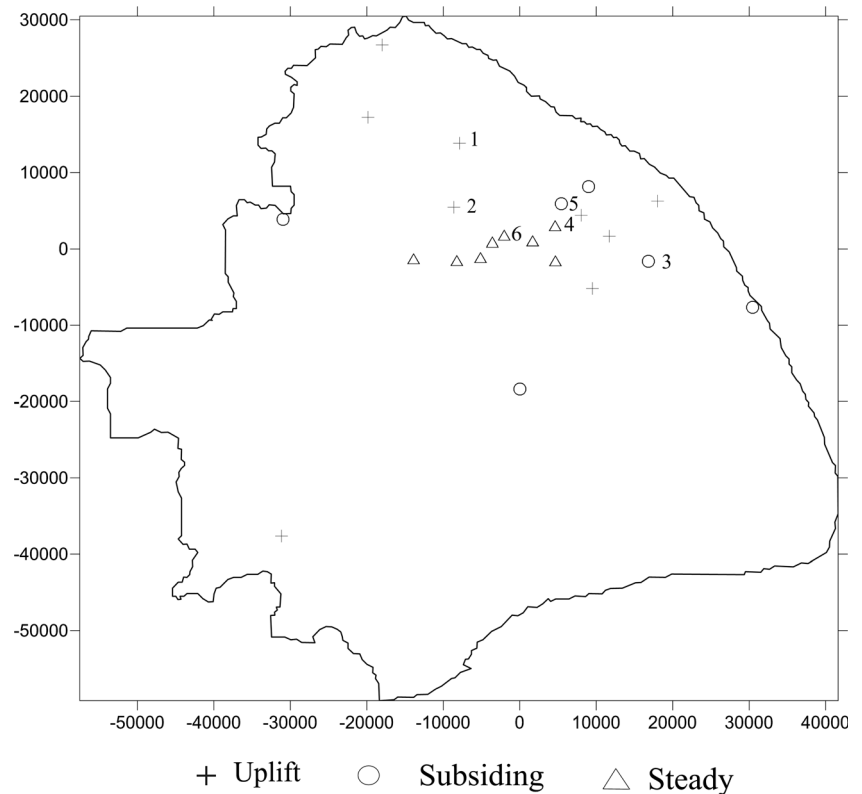
installed in the late 1990s and have been measuring compaction since 1998. By the mid-2012, land subsidence in the most central area of Shanghai had been arrested and, at some places, land uplift had clearly occurred (Fig. 9). The earliest land uplift occurred at extensometer group 1 in the northern part in 2003, where the cumulative uplift had reached 30.59 mm

by the mid-2012. Most uplift in Shanghai started in the period of 2008 to 2011. For instance, land surface at extensometer group 2 subsided till 2008 and then uplifted by 4 mm by mid-2012. Land surface at several extensometer groups still subsided, but the subsidence rate has decreased. The maximum average yearly subsidence rate in the period from January

Table 2 Stages of land subsidence in Shanghai

Stage		Average yearly rate of subsidence (mm/year)
Rapidly developing (1921–1965)	Increasing (1921–1948)	23.6
	Dramatically increasing (1949–1956)	40.3
	Very dramatically increasing (1957–1961)	99.4
	Slowly increasing (1962–1965)	61.3
Controlling (1966–2011)	Rebounding (1966–1971)	–3.4
	Slightly increasing (1972–1989)	3.2
	Increasing (1990–2003)	12.7
	Slowly increasing (2004–2008)	6.2
	Coming to end (2009–2011)	1.3

Fig. 9 Land level trend at extensometer groups in Shanghai in the middle of 2012 (the unit of coordinates: m)



2009 to May 2012 is 6.1 mm/year, which occurred at extensometer group 3. Compared with the continuous increase of groundwater level in aquifers, land uplift lags behind by at least a decade at some sites.

As far as the individual hydrostratigraphic units are concerned, the contribution of each unit to the total land subsidence and uplift changes in different stages. On the basis of available data on compaction for individual units, the percentage of compaction for a specific unit in total subsidence and uplift can be calculated. During the 1981–1989 stage, the ground surface subsided again following a period of rebound. The compaction occurred primarily in the first and second soft soil layers. Then the pumpage increased greatly and was primarily from the fourth confined aquifer. Correspondingly, the fourth confined aquifer became the main subsidence layer during the 1990–2003 and 2004–2008 stages. With increasing artificial recharge and decreasing pumpage, groundwater levels in all confined aquifers have significantly increased. As a result, most of the deeper soil units expanded in the stage 2009–2011. Even at extensometer group 3 where the subsidence rate is maximal, the hydrostratigraphic units below the third confined aquifer have rebounded; however, compaction still occurred within the shallow soft soil layers. When the expansion of some units outpaces the compaction of the other units, land uplift will occur. Due to the space limitations, Table 3 merely shows the percentage of the compaction of individual hydrostratigraphic units in the total land subsidence

in different stages at extensometer groups 4–6, where the total land subsidence in each stage is indicated in Table 4. At these sites, the shallow soft soil layers and the fourth confined aquifer have continuously subsided, while other units expanded. At extensometer group 6, for example, land subsidence has nearly been arrested, and the average is only 0.07 mm/year in the stage from 2009 to 2011, during which the compaction of the fourth confined aquifer is 4.3 mm. In summary, most deep hydrostratigraphic units have rebounded, but the shallow units, especially the first and second soft soil layers, continue to compact due to their high compressibility, low permeability, and significant creep behavior, and the fourth aquifer continues compacting in some places; however, their compaction rate has clearly decreased in recent years. If the groundwater level follows the current rising trend or remains steady for a longer time, the shallow units and the fourth aquifer will stop compacting, and some rebound may occur.

With groundwater level changing, individual units have responded differently: some units compacted and others expanded. Even aquifers deformed differently under a similar rising pattern of groundwater level—for instance, with the groundwater levels in the second and fourth confined aquifers increasing after 1998, the second aquifer almost expanded immediately, but the fourth aquifer continued to compact for more than 10 years and did not reach a stable state until 2012 (Fig. 10). The reason for the different deformation characteristics of these two aquifers is that they have experienced

Table 3 Percentage of compaction for individual hydrostratigraphic units in the total land subsidence at extensometer groups for given periods. *Positive values indicate compaction and negative values indicate expansion; data regarding aquifers are in italics*

Hydrostratigraphic unit	Extensometer group 4				Extensometer group 5				Extensometer group 6						
	Depth (m)	1981–1989	1990–2003	2004–2008	2009–2011	Depth (m)	1981–1989	1990–2003	2004–2008	2009–2011	Depth (m)	1981–1989	1990–2003	2004–2008	2009–2011
Unconfined aquifer	0–3	37.7	3.2	5.0	23.9	0–7	7.1	6.0	10.2	27.4	0–15	16.4	1.7	15.7	1,281.0
1st aquitard: 1st soft soil layer	3–42 ^a	57.4 ^a	14.9 ^a	24.6 ^a	111.4 ^a	7–20	45.8	14.7	34.2	65.9	15–26 ^a	22.9 ^a	2.7 ^a	6.6 ^a	547.6 ^a
1st aquitard: 2nd soft soil layer						20–24	3.4	3.2	9.8	14.1					
1st aquitard: 2nd hard soil layer	absent	–	–	–	–	24–30	–2.9	0.7	2.6	2.1	26–44 ^b	–0.7 ^b	0.6 ^b	–2.7 ^b	–76.2 ^b
1st confined aquifer	42–50	–0.6	–1.6	1.2	–21.1	30–48	7.1	3.5	6.0	7.1					
2nd aquitard	50–73	5.3	2.3	–0.1	–12.8	48–88	18.8	8.4	3.0	–0.8	44–79	17.5	16.6	24.3	0
2nd confined aquifer	73–149 ^c	1.2 ^c	0.8 ^c	–1.0 ^c	–21.0 ^c	88–153 ^c	0.9 ^c	3.3 ^c	–1.5 ^c	–9.9 ^c	79–111	–0.8	2.2	–6.0	352.4
3rd aquitard											111–124	3.6	–0.6	7.4	–1,347.6
3rd confined aquifer											124–149	–3.8	7.9	–11.6	–490.5
4th aquitard	149–179	2.6	12.7	13.6	–1.8	153–174	2.4	8.9	–0.2	–6.5	149–165	6.3	9.0	6.8	–214.3
4th confined aquifer	179–243	15.3	64.6	55.5	50.1	174–239	10.0	62.6	33.1	9.4	165–211	22.9	53.3	54.1	2,047.6
5th aquitard ^d	243–345	–19.0	3.1	1.1	–28.6	239–333	7.5	–11.4	2.8	–9.0	211–295	15.5	6.4	5.3	–2,000.0
5th confined aquifer ^d															
6th aquitard ^d															

^a 1st aquitard (1st and 2nd soft soil layers combined)

^b Combined 1st aquitard (2nd hard soil layer) and 1st confined aquifer

^c Combined 2nd confined aquifer, 3rd aquitard and 3rd confined aquifer

^d All data combined

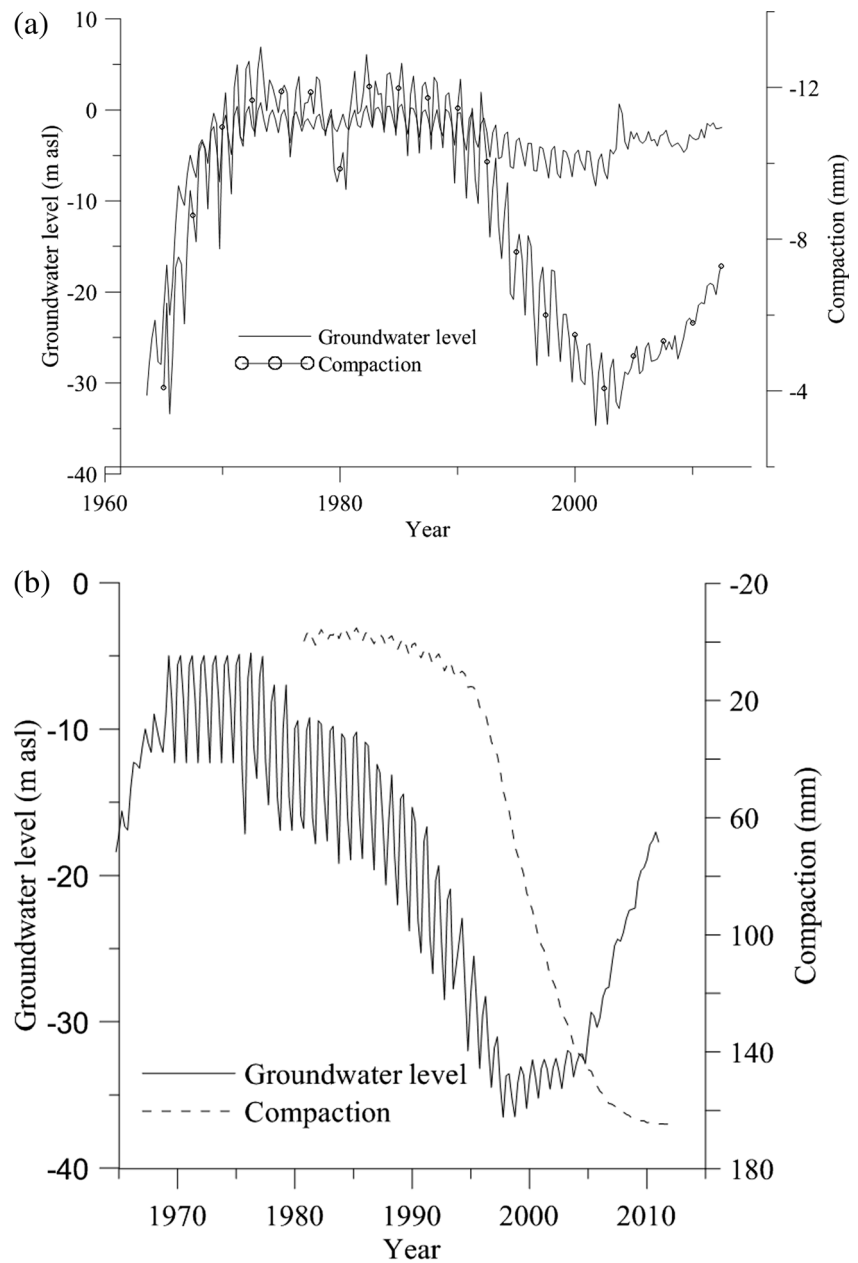
Table 4 Total land subsidence in individual periods

Extensometer group	Land subsidence (mm)			
	1981–1989	1990–2003	2004–2008	2009–2011
4	99.28	491.81	64.04	6.49
5	36.17	221.50	71.43	14.61
6	25.99	181.49	34.13	0.21

different modes of changing groundwater level. The groundwater level in the second aquifer was always higher than the lowest level it reached in the early 1960s, while the groundwater level in the fourth aquifer was lower than the lowest level it reached in the 1960s after 1989. Figure 10a shows

the history of groundwater level in the second confined aquifer and its compaction at extensometer group 5, where the second and fourth confined aquifers are mainly composed of sands, with little clay/silt lenses, according to the borehole log. The compaction follows closely with the change of

Fig. 10 History of compaction and groundwater level at extensometer group 5. **a** The second confined aquifer, **b** the fourth confined aquifer



groundwater level. When the groundwater level increased after 2001, the unit rebounded immediately. Figure 10b is the groundwater level in the fourth confined aquifer and its corresponding compaction from 1980 to 2012 at the same site. Before 1989, the unit clearly rebounded when groundwater rose in a yearly cycle; however, the unit did not expand but continued compacting after 1989 even when the groundwater level increased. The compaction of the unit nearly stopped in 2010 after it had approximately experienced a 10-year rise of groundwater level; additionally, the expansion has not occurred yet and the compaction obviously lags behind the change in the groundwater level for this unit. Consequently, the hydrostratigraphic units have complex deformation characteristics under changing groundwater levels resulting from long-term groundwater extraction. Even aquifers do not always deform elastically and expand immediately after the groundwater level in them increases.

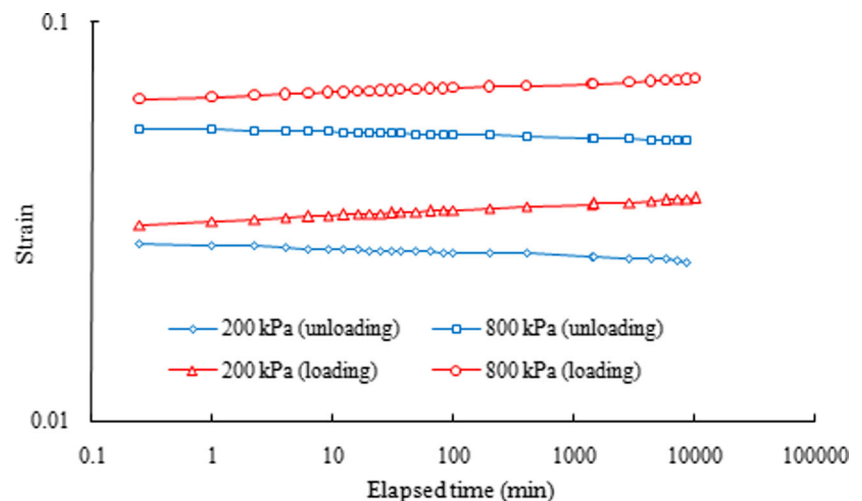
Laboratory tests on aquifer sands

In order to comprehensively understand the expansion of soils under the condition of decreasing effective stress, some laboratory tests were conducted. Clay soils have low permeability. When they are loaded or unloaded suddenly, it will take a long time for the resultant extra pore-water pressure in them to dissipate completely, during which time the effective stress in soils changes with the elapsed time; hence, the measured deformation includes both consolidation and creep deformation, which cannot be separated from each other in a laboratory. Comparatively, saturated sands have great permeability, and the extra pore-water pressure due to loading and unloading dissipates and the consolidation finishes very soon after the loading is suddenly

applied or removed. Then the effective stress in sand samples remains nearly constant. Sand samples are therefore used here to assure that the measured time-dependent deformation very soon after loading or unloading is the creep deformation under a constant effective stress (Lade and Liu 1998; Murayama et al. 1984; Pestana and Whittle 1998). The test samples were acquired from the aquifers of Shanghai, and odometers were used in the tests. The loading was first applied suddenly on the sample, and the compression was documented until the rate of deformation was less than 0.005 mm/day. Then the loading was removed completely and the expansion was documented until the rate was less than 0.005 mm/day. The details of the tests were published earlier (Zhang et al. 2009); thus, only some relevant and necessary information is mentioned here.

Figure 11 is the documented vertical strain and time of two sand samples under loading and unloading in odometer tests. The applied loading is 800 and 200 kPa for the two samples, respectively, and then loading is removed completely. Figure 11 shows that both compression and expansion do not complete immediately after loading or unloading but increase with the elapsed time. This time-dependent deformation occurs under constant effective stresses and results from soil creep. The test results also show that some of the creep deformation for sand is recoverable, but it is much smaller than the irrecoverable deformation in a loading and unloading cycle. Even though the creep of sands is weaker than that of clays, the creep deformation of a sand unit will be remarkable if the thickness of the unit is great enough. According to the test results, sand does not deform elastically but plastically and by creep, and approximately 30% compression can be recovered for the tested sand samples under a loading-unloading cycle. For example, under the loading-unloading

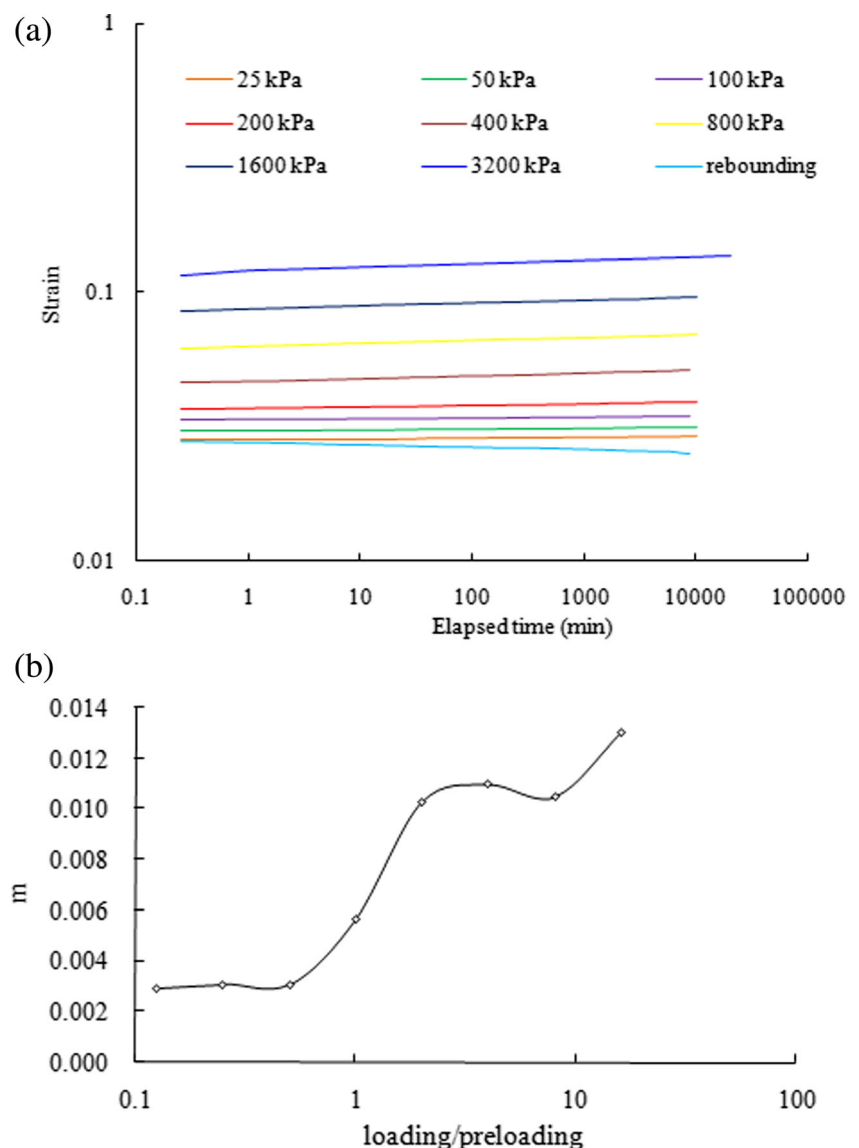
Fig. 11 Creep curves under loading and unloading in a double logarithmic space



cycle of 200 kPa, the elastic deformation is 23.2%, plastic deformation is 62.6%, and the creep deformation is 14.2%. Consequently, only a small portion of compaction is recoverable when the groundwater level increases in aquifers, and both compaction and expansion do not complete immediately when groundwater level decreases or increases in aquifer units. On the other hand, the creep of sand samples is affected greatly by the preloading on them. For instance, the sample was first applied a loading of 200 kPa, and the loading was removed completely when the rate of compression was less than 0.005 mm/day. The expansion was documented till the rate of expansion was less than 0.005 mm/day. Then the loading was applied in multiple stages. When the loading surpasses the preloading, the slope of the creep curve in a double logarithmic space becomes much greater, meaning stronger creep; otherwise, the slope is much smaller, as shown in

Fig. 12a. The relationship between the slope m and the ratio of current loading to preloading is shown in Fig. 12b. When multiple loading-unloading cycles are applied, the slope of creep curves decreases with the increasing number of cycles. The slope value for the first loading is much greater than those for the following loading cycles, but there is no great change in the slope of creep curves after the second loading cycle. Moreover, the rebounding deformation is nearly the same in each cycle (Zhang et al. 2012). Therefore, when the groundwater level in an aquifer unit is lower than its historically lowest value, the unit will exhibit much more compressibility and creep. Otherwise, it will have less creep deformation and deform closely following the changing groundwater level. As for aquitard units, they often have less recoverable and clearer creep deformation under the same conditions of loading and unloading.

Fig. 12 **a** Creep curves under multiple-stage loading in a double logarithmic space. **b** Relationship between slope, m , and the ratio of current loading to preloading



Discussion

Mechanical model of hydrostratigraphic units

On the basis of the comprehensive analysis of field and laboratory data, a double-yielding visco-elasto-plastic model was proposed, as shown in Fig. 13 (Zhang et al. 2012), which can better represent the deformation characteristics of hydrostratigraphic units under long-term groundwater withdrawal. The model includes two yielding stresses. When the effective stress in aquifer units is smaller than the first yielding stress, elastic and visco-elastic deformation will occur. When the effective stress in aquifer units is greater than the first yielding stress but smaller than the second yielding stress, the unit will have elastic, plastic, and visco-elastic deformation. When the effective stress is greater than the second yielding stress, the unit will have visco-plastic deformation. When the effective stress decreases, the elastic and visco-elastic deformation can recover, but plastic and visco-plastic deformation is unrecoverable. The first yielding stress is no greater than the second in any of the cases. The total deformation consists of elastic, plastic, visco-elastic, and visco-plastic strain. From the aforementioned test results, it can be inferred that elastic and visco-elastic strain is much smaller than the irrecoverable plastic and visco-plastic strain. For the model, the relationship of stress, strain, and time is (Zhang et al. 2015)

$$\begin{cases} \varepsilon = \varepsilon_1 + \varepsilon_2 + \varepsilon_3 \\ \varepsilon_1 = \frac{\sigma}{E_1} + \frac{\langle \sigma - \sigma_{01} \rangle}{H_1} \\ E_2 \varepsilon_2 + \eta_1 \dot{\varepsilon}_2 = \sigma \\ H_2 \varepsilon_3 + \eta_2 \dot{\varepsilon}_3 = \langle \sigma - \sigma_{02} \rangle \end{cases} \quad (1)$$

in which

$$\langle \sigma - \sigma_{0i} \rangle = \begin{cases} 0 & \sigma \leq \sigma_{0i} \\ \sigma - \sigma_{0i} & \sigma > \sigma_{0i} \end{cases} \quad (i = 1, 2) \quad (2)$$

where E_1 and E_2 are the elastic moduli for springs S1 and S2, respectively, MPa; H_1 and H_2 are the plastic moduli for plastic elements P1 and P2, respectively, MPa; η_1 and η_2 are the viscosity for dashpots C1 and C2, respectively, MPa-year; ε is the strain; σ is the effective stress, MPa; ε_1 is the elastic and plastic strain; ε_2 is the visco-elastic strain; ε_3 is the visco-plastic strain; $\dot{\varepsilon}_2$ is the derivative of visco-elastic strain with respect to time; $\dot{\varepsilon}_3$ is the derivative of visco-plastic strain with respect to time; σ_{01} is the first yielding stress, MPa; σ_{02} is the

second yielding stress, MPa. Under a constant effective stress σ , given the initial condition $\varepsilon|_{t=0} = \frac{\sigma}{E_1} + \frac{\sigma - \sigma_{01}}{H_1}$, the strain at time t is

$$\varepsilon = \frac{\sigma}{E_1} + \frac{\sigma}{H_1} \left(1 - \frac{\sigma_{01}}{\sigma}\right) + \frac{\sigma}{E_2} \left(1 - e^{-\frac{E_2}{\eta_1}t}\right) + \frac{\sigma}{H_2} \left(1 - \frac{\sigma_{02}}{\sigma}\right) \left(1 - e^{-\frac{H_2}{\eta_2}t}\right) \quad (3)$$

Supposing that the stress is completely removed when the elapsed time is t_1 under the effective stress σ , and that the superposition principle is applied, then the strain at time t ($t > t_1$) is

$$\varepsilon = \frac{\sigma}{H_1} \left(1 - \frac{\sigma_{01}}{\sigma}\right) + \frac{\sigma}{E_2} \left(1 - e^{-\frac{E_2}{\eta_1}t_1}\right) e^{-\frac{E_2}{\eta_1}(t-t_1)} + \frac{\sigma}{H_2} \left(1 - \frac{\sigma_{02}}{\sigma}\right) \left(1 - e^{-\frac{H_2}{\eta_2}t_1}\right) \quad (4)$$

When both σ_{01} and σ_{02} equal zero as is the case in virgin loading and then unloading, the change of strain with time can be obtained for a different time t_1 according to Eqs. (3) and (4), as shown in Fig. 14. It shows that the strain at a given time t ($t > t_1$) in a loading and unloading cycle increases with the increasing time t_1 . This suggests that the effect of artificial recharge on land subsidence mitigation will be better if it is conducted earlier.

In order to investigate the most sensitive factors that control the strain, the sensitivity of the strain at time t ($t > t_1$) to parameters is analyzed from Eqs. (3) and (4). Figure 15 shows the effects of the ‘change in individual parameters’ on the strain at 3 years with t_1 being 2 years. One parameter value is changed at a time in the sensitive analyses. The basic values for parameters are: $E_1 = 1,600$ MPa, $E_2 = 800$ MPa, $H_1 = 200$ MPa, $H_2 = 300$ MPa, $\eta_1 = 350$ MPa-year, and $\eta_2 = 250$ MPa-year. Because the elastic deformation can completely recover in a loading and unloading cycle, the parameter E_1 has no effect on the strain at time t . The time-independent and irrecoverable plastic deformation is determined by the parameter of H_1 in a loading and unloading cycle; thus, it is the most important factor for the strain at time t . The strain decreases with increasing value of H_1 . The visco-plastic deformation is time-dependent and irrecoverable, and related to the parameters of H_2 and η_2 . The strain changes inversely with the parameter H_2 . The parameter η_2 , especially for its greater values, has an important effect on the strain, and the strain decreases with increasing η_2 . The parameter E_2 has a remarkable impact on the visco-elastic strain which decreases with increasing value

Fig. 13 Double-yielding visco-elasto-plastic model (Zhang et al. 2012)

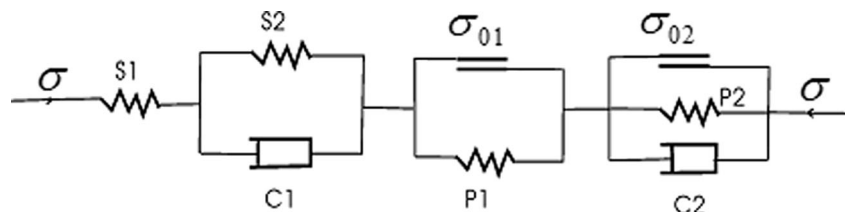
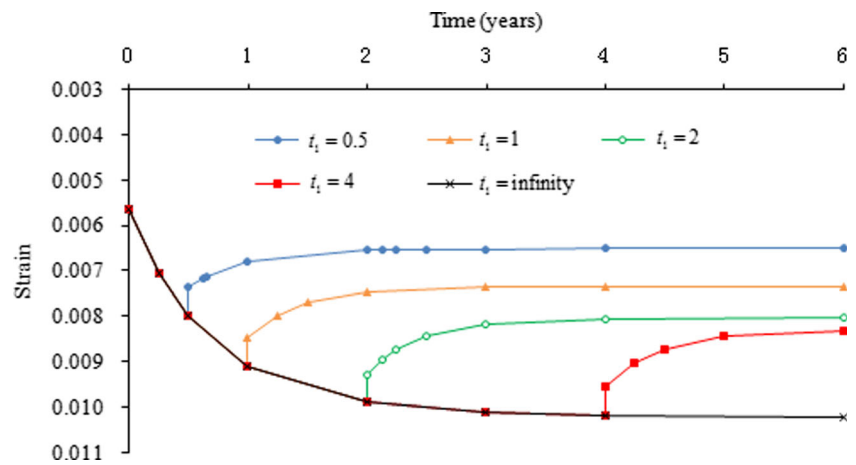


Fig. 14 Compaction strain for a loading and unloading cycle



of this parameter. The parameter η_1 affects the rate of visco-elastic strain but it has no impact on the ultimate visco-elastic strain. The visco-elastic strain can completely recover when unloading if the elapsed time is long enough; therefore, the parameters of E_2 and η_1 do not affect the strain at time t , which is much greater than the time t_1 .

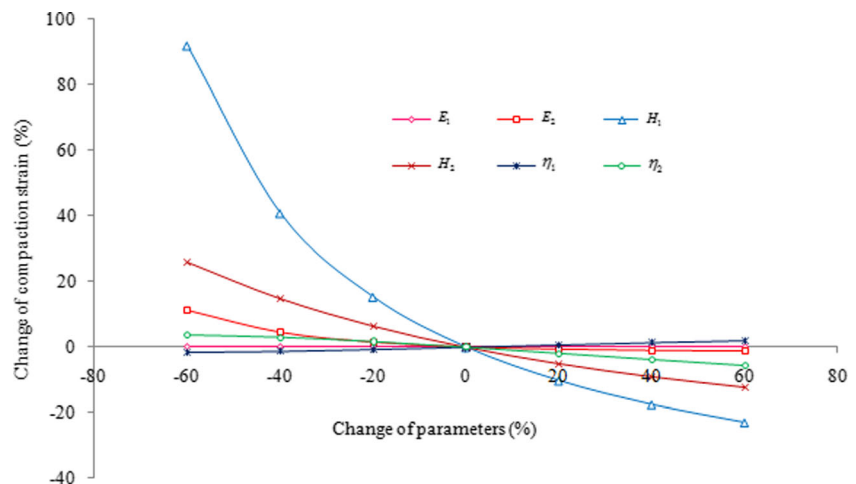
Mechanism of land uplift in Shanghai

There have been two periods when the yearly average groundwater level in Shanghai continued to rise significantly: one was approximately from the early 1960s to the 1970s, the other has approximately been from the end of 1990s to the present. The great rise of the groundwater level in both periods has led to land uplift to some extent. Due to the lack of detailed compaction for individual hydrostratigraphic units obtained from extensometer groups in the first period, the present analyses are based on the second one. The groundwater levels in all confined aquifers have increased since the late 1990s; however, each aquifer unit presents different deformation characteristics because it has experienced different changing patterns of groundwater level.

The first to third confined aquifer units have experienced the groundwater level change of mode A. Taking the second confined aquifer as an example, it reached its historically lowest level in the early 1960s, meaning that it was subjected to the maximum effective stress at that time. The visco-plastic compaction caused by the first-stage decline of groundwater level had nearly come to an end by the early 1980s when the groundwater level began to decrease for the second time. The visco-plastic compaction can be ignored and the aquifer compacted closely following the change of groundwater level. Therefore, when the groundwater level rose in the second period, the three confined aquifer units almost expanded immediately. In spite of this, the rebound is not great because of less elastic and visco-elastic deformation for sands and the small change in groundwater level within these units in this period.

The fourth and fifth aquifer units have experienced the groundwater level change of mode B. The groundwater level in the second cycle decline was lower than that in the first cycle; thus, the aquifers had additional visco-plastic compaction. The visco-plastic compaction did not stop when the groundwater level rose in the second period. Moreover, it

Fig. 15 Effects of change in individual parameters on the compaction strain after a loading-unloading cycle



outpaced the elastic and visco-elastic rebound, causing the aquifer unit to continue compacting even though the groundwater level rose. With the passing of time, the rate of visco-plastic compaction decreased. When the elastic and visco-elastic rebound outpaced the visco-plastic compaction, the aquifer unit would rebound. The compaction of the aquifer clearly lags behind the change of the groundwater level in it. Consequently, it is not always the case for aquifer units to rebound closely following the rise of groundwater level in them and to recover completely when the effective stress in them reduces.

Due to much lower permeability, the change of the groundwater level within aquitard units lags behind that in their neighboring discharge and recharge aquifer unit. On the other hand, aquitard units, consisting of soft clay soil, often have stronger visco-plastic compaction than aquifer units (Zhang et al. 2011), which leads to the great lagging of rebound of such aquitard units behind the recovery of groundwater level in their neighboring aquifers.

Land subsidence is the sum of compaction of intervening aquifer and aquitard units. Land uplift occurs only when the expansion of all rebounding units is greater than the compaction of all compacting units. Whether ground surface uplifts or not depends on many factors such as changing patterns of groundwater level, deformation characteristics of soils that consist of aquifer and aquitard units, and the permeability and the thickness of units.

Conclusions

Excessive groundwater withdrawal has caused severe land subsidence in Shanghai. It has been alleviated by raising groundwater level in hydrostratigraphic units through artificial water recharge and restriction on groundwater pumpage. On the basis of field and laboratory data, the characteristics and mechanisms of land subsidence and uplift are analyzed and discussed, and the following conclusions can be drawn.

Under the condition of long-term groundwater withdrawal, the deformation of both aquifer and aquitard units consists of elastic, plastic, visco-elastic, and visco-plastic components. When the groundwater level in the units rises, the elastic deformation can recover immediately, but the recovery of visco-elastic deformation is time-dependent. The plastic and visco-plastic deformation is irrecoverable. The recoverable deformation is only a small portion of the total deformation for both aquitard and aquifer units, especially when the groundwater level in the units is lower than the historically lowest values. For a certain groundwater extraction and resultant change in groundwater level, land subsidence increases and land uplift decreases with the decreasing plastic modulus and visco-plastic modulus of the units.

When groundwater level in aquifer units rises, whether their expansion occurs immediately or not depends on the changing modes of groundwater level they have experienced. There are two changing modes of groundwater level in Shanghai from the very beginning of groundwater extraction to the present. The aquifers rebound immediately with the increasing groundwater level in the second cycle of mode A, but their expansion lags behind in that of mode B. Aquitard units often have lower permeability and greater creep deformation, and the change of groundwater level in them lags behind that in the neighboring aquifer units; thus, their expansion always lags behind the rise of groundwater level in the aquifer units. The lagging becomes more obvious with smaller permeability and greater creep of the units.

The change of land elevation is the sum of compaction of the intervening aquifer and aquitard units. Each unit experiences a different changing mode of groundwater level and exhibits different deformation characteristics; also, some units may compact and others may rebound. If the expansion of all rebounding units is greater than the compaction of all compacting units, land uplift occurs; otherwise, land subsides. The change of land displacement from subsidence to uplift often lags behind the start of the continuous rise of groundwater level in aquifer units due to the artificial recharge and/or the limitation of pumpage. The lagging is attributed not only to the visco-plastic deformation and the consolidation deformation of aquitard units, but also to the visco-plastic deformation of the aquifer units.

Artificial recharge and limitation of pumpage are effective measures for controlling land subsidence. As a result of these measures, land subsidence in most parts of Shanghai has been arrested and land uplift has even occurred at some localities. However, earlier artificial recharge is necessary to keep groundwater levels in all aquifer units above their historically lowest values all the time and/or to make the units develop less visco-plastic compaction if a more effective outcome is expected. In such a case, the irrecoverable and lagging visco-plastic compaction will be decreased greatly and the change of land surface elevation is small.

Acknowledgements The authors gratefully acknowledge the constructive comments and suggestions from Prof. Maria-Theresia Schafmeister, an anonymous associate editor, an anonymous reviewer, and Dr. Devin L. Galloway, which were all very helpful for the authors to improve the quality of this manuscript.

References

- Chen CT, Hu JC, Lu CY, Lee JC, Chan YC (2007) Thirty-year land elevation change from subsidence to uplift following the termination of groundwater pumping and its geological implications in the Metropolitan Taipei Basin, Northern Taiwan. *Eng Geol* 95:30–47

- Galloway DL, Jones DR, Ingebritsen SE (1999) Land subsidence in the United States. U S Geol Surv Circ 1182, 177 pp
- Gong SL (2009) Change of groundwater seepage field and its influence on development of land subsidence in Shanghai (in Chinese). *J Water Resour Water Eng* 20(3):1–6
- Hoffmann J, Zebker HA, Galloway DL, Amelung F (2001) Seasonal subsidence and rebound in Las Vegas Valley, Nevada, observed by synthetic aperture radar interferometry. *Water Resour Res* 37(6): 1551–1566
- Kosloff D, Scott RF, Scranton J (1980) Finite element simulation of Wilmington oil field subsidence: I. linear. *Tectonophysics* 65:339–368
- Lade PV, Liu CT (1998) Experimental study of drained creep behavior of sand. *J Eng Mech* 124(8):912–920
- Leake SA (1991) Simulation of vertical compaction in models of regional groundwater flow. In: Johnson AJ (ed) *Land subsidence (Proceedings of the Fourth International Symposium on Land Subsidence)*. IAHS Publ. no. 200, IAHS, Wallingford, UK, pp 565–574
- Murayama S, Michihiro K, Sakagami T (1984) Creep characteristics of sands. *Soils Foundations* 24(2):1–15
- Pestana JM, Whittle AJ (1998) Time effects in the compression of sands. *Geotechnique* 48(5):695–701
- Schmidt DA, Bürgmann R (2003) Time-dependent land uplift and subsidence in the Santa Clara valley, California, from a large interferometric synthetic aperture radar data set. *J Geophys Res* 108(B9):2416
- SGEAEB (Shanghai Geological Environmental Atlas Editorial Board) (2002) *Shanghai geological environmental atlas* (in Chinese). Geological Publishing House, Beijing, 143 pp
- Teatini P, Castelletto N, Ferronato M, Gambolati G, Tosi L (2011) A new hydrogeologic model to predict anthropogenic uplift of Venice. *Water Resour Res* 47:W12507
- Teatini P, Tosi L, Strozzi T, Carbognin L, Cecconi G, Rosselli R, Libardo S (2012) Resolving land subsidence within the Venice Lagoon by persistent scatterer SAR interferometry. *Phys Chem Earth* 40–41: 72–79
- Zhang AG, Wei ZX (2005) *Land subsidence in China* (in Chinese). Shanghai Science and Technology Press, Shanghai, 240 pp
- Zhang Y, Xue YQ, Li QF (2003) Current prominent subsidence layer and its deformation properties in Shanghai (in Chinese). *Hydrogeol Eng Geol* 30(5):6–11
- Zhang Y, Xue YQ, Wu JC, Liu YT, Pu XF (2009) Experimental research on creep of Shanghai sands (in Chinese). *Rock Soil Mech* 30(5): 1226–1230
- Zhang Y, Xue YQ, Wu JC, Wang HM, He JJ (2012) Mechanical modeling of aquifer sands under long-term groundwater withdrawal. *Eng Geol* 125:74–80
- Zhang Y, Xue YQ, Wu JC, Ye SJ, Li QF (2007) Stress–strain measurements of deforming aquifer systems that underlie Shanghai, China. *Environ Eng Geosci* 13(3):217–228
- Zhang Y, Xue YQ, Wu JC, He JJ, Wang HM (2011) Experimental study of creep deformation of saturated clay (in Chinese). *Rock Soil Mech* 32(3):672–676
- Zhang Y, Xue YQ, Wu JC, Wang ZC (2015) Compaction of aquifer units under complex patterns of changing groundwater level. *Environ Earth Sci* 73:1537–1544
- Zhou X, Burbey TJ (2014) Deformation characteristics of a clayey interbed during fluid injection. *Eng Geol* 183:185–192